A Cognitive TV White Space-Broadband Power Line MIMO System for Indoor Communication Networks

Mohammad Heggo*†, Xu Zhu*§, Sumei Sun† and Yi Huang*

***Abstract*—Broadband power line communication (BPLC) is a promising solution to satisfy the growing data rate demands for broadband indoor communication networks. However, the BPLC transmission power spectral density (PSD) is restricted in the very high frequency (VHF) band to avoid harmful interference to the existing wireless services. In this paper, a new hybrid system is proposed utilizing BPLC and cognitive radio over TV white space (TVWS) to enhance the system capacity over BPLC in VHF, forming a VHF TVWS BPLC multiple-input multiple-output (MIMO) system. An iterative precoding algorithm is proposed to satisfy the interference limit at the TV primary user (PU) receiver (Rx) and enhance the ergodic capacity. Moreover, a power allocation algorithm is developed for the MIMO system to achieve the maximum ergodic capacity subject to the average total power constraint and limit of interference to TV PU. Simulation results demonstrate the significant enhancement in the achieved capacity by our proposed system in the VHF band compared to both previous cognitive and hybrid BPLC systems.**

***Index Terms*—Broadband communication, Cognitive radio, Indoor communication, MIMO, VHF.**

I. Introduction

Broadband power line communication (BPLC) has drawn the attention of the researchers in the last decade as it offers the indoor networks a high speed cost-effective solution [1]. However, the electromagnetic compatibility (EMC) with wireless services remains a crucial problem for BPLC transceivers [2] [3]. Hence, in ITU-T G.hn, HomePlug AV2 and IEEE 1901 standards [4] [5], the BPLC transmission power spectral density (PSD) in the very high frequency (VHF) band is restricted to -85 dBm/Hz. The latter constraint significantly limits the capacity of the BPLC in the VHF band and hence is considered as a crucial problem for the BPLC.

Enhancing the BPLC capacity and satisfying the interference limit with wireless devices had been approached in the literature using three methods: 1) multiple-input multiple-output (MIMO) BPLC as in [4] and [6], 2) cognitive BPLC as in [7]–[11], and 3) hybrid wireless BPLC as in [12]. Although MIMO BPLC can offer some enhancement of the system capacity, it still cannot achieve high ergodic capacity in the VHF band due to the transmitter PSD mask forced by [5]. For cognitive BPLC, the BPLC transmitter (Tx) uses its coupling circuit to sense the spectrum before transmission to avoid interference with existing wireless services, and hence improve the overall ergodic capacity of the system. The main drawback in the cognitive BPLC is the weak reception capability of the BPLC coupling circuit to VHF wireless signals, due to the near field coupling loss between the BPLC and the VHF wireless channels as previously addressed in [2]. Besides, even for the MIMO cognitive BPLC, the coupling circuit itself is considered as a passive circuit device that can increase the coupling loss of the wireless signal. Also, weak coupling between the power line signals and the wireless VHF band can lead to a long sensing time that yields a capacity loss.

As for hybrid wireless BPLC, WiFi was proposed in [12] to enhance the capacity of BPLC by building up a hybrid BPLC WiFi transceiver. The solution relies on the cooperation between the BPLC transceiver in the frequency band below 30 MHz with a transmitter PSD of -55 dBm/Hz [5] and the WiFi transceiver in the 2.45 GHz band with transmission power limit of 23 dBm [13], which is equivalent to -50 dBm/Hz for 20 MHz bandwidth. However, when the BPLC transceiver is used in the frequency band beyond 30 MHz, it suffers a lower transmission PSD limit of -85 dBm/Hz [5] while the WiFi transceiver in the 2.45 GHz band still has the same transmission power limit of 23 dBm. This limit difference results in allocation of most transmission power to the WiFi channel which suffers a higher path loss compared to the BPLC channel. This yields overall capacity degradation, compared to the BPLC WiFi capacity in the frequency band below 30 MHz.

Measurements performed by the Federal Communication Committee (FCC) had shown that large portions of the TV spectrum are locally or temporarily unused [14]. Those portions are known as TV white space (TVWS). According to the FCC TVWS standard [14], unlicensed users are allowed to access the TVWS with transmission power up to 100 mW in the VHF band from 54 MHz to 216 MHz and in the ultra-high frequency (UHF) band from 470 MHz to 806 MHz. Furthermore, TVWS suffers lower path loss than the WiFi bands at 2.45 GHz and 5 GHz [15] [16]. Hence, more attention is paid to exploiting the TVWS in high speed indoor network applications such as TV video streaming [17]. In [18], we investigated the ergodic capacity of the hybrid TVWS BPLC communication in the VHF band. This provides a preliminary feasibility study of the cooperation, which relies

This paper was presented in part at the IEEE VTC Fall 2016.

*Department of Electrical Engineering and Electronics, The University of Liverpool, Liverpool L69 3GJ, UK.

†Institute for Infocomm Research, Agency for Science, Engineering and Research, Singapore.

§Corresponding author email address: xuzhu@liverpool.ac.uk.

on the channel path loss regardless of the complex channel gain variation and also the availability of the primary user (PU) channel state information (CSI).

In this paper, a new cooperative system between BPLC and TVWS in the VHF band 54 MHz - 88 MHz is proposed. Our work is different in the following aspects. First, the proposed system improves significantly the VHF BPLC capacity through adding the wireless TVWS channel and using the advantage of MIMO channel. Our system is different from the previous MIMO cognitive BPLC system in [4] since the TVWS BPLC Tx can access the VHF band with lower Tx PSD constraints using the TVWS standard [14], which enhances significantly the overall system capacity. It is worth mentioning that, to the best of our knowledge, this is the first work to propose a cognitive BPLC solution that complies with the TVWS standard. The addition of wireless antenna to cognitive BPLC is essential to enable our TVWS BPLC Tx to sense the TV PU at very low power level of -114 dBm, which satisfies the requirement of the TVWS standard [14]. This addition of the TVWS antenna solves the problem of coupling loss that exists in the aforementioned cognitive BPLC solutions. Second, the interference to other wireless services is mitigated using a proposed iterative precoding technique at the Tx. The proposed algorithm takes the advantage of the multiple-input single-output (MISO) channel between the TVWS BPLC Tx and the TV wireless receiver (Rx). Third, an efficient power allocation algorithm is derived for the MIMO system in order to achieve maximum ergodic capacity for each subcarrier. Fourth, compared to the hybrid BPLC WiFi system [12], our system offers a more cost-effective hybrid solution. This is due to the elimination of the RF up- and down-converters needed for the WiFi transceiver.

The paper is organized as follows. In Section II, the proposed system model including the channel model is presented. In Section III, cognitive spectrum access is addressed, including an iterative precoding technique and MIMO spectrum sensing. In Section IV, the power allocation for the MIMO channel is presented. In Section V, the capacity simulation results of our proposed system are compared with BPLC WiFi and MIMO BPLC. Finally, in Section VI the paper is concluded.

Notations: $\mathbb{E}\{.\}$ denotes the expectation operator, $\lceil x \rceil^+$ denotes $\max(0, x)$, vectors are represented by boldface letters and the Hermitian of a matrix $\mathbf{A}$ is $\mathbf{A}^\dagger$, and the conjugate transpose of a vector $\mathbf{v}$ is $\mathbf{v}^\dagger$. $\mathbf{I}$ denotes the identity matrix.

II. System Model

A. MIMO TVWS BPLC Model

The proposed TVWS BPLC system model is illustrated in Fig. 1. The TV PU activity (*i.e.*, presence or absence) in the TVWS band is assumed to be known at the TVWS BPLC Tx due to access to a geolocation database as stated in [14]. In this paper, we propose two modes of operation for the TVWS BPLC system according to the available CSI. The CSI of the PU Rx in our work is defined as the interference complex channel gain vector $\mathbf{g}$ between the TVWS BPLC Tx and the PU Rx. The two proposed modes are: 1) Opportunistic Mode: The CSI of the PU Rx is available to the TVWS BPLC transceiver; 2) Non Opportunistic Mode: The CSI of the PU Rx is unavailable to the TVWS BPLC transceiver. The CSI in the opportunistic mode can be obtained using the sensing method in [19]. Obtaining the CSI between the TVWS BPLC Tx and the PU Rx using the method in [19] relies on the permission of the PU network given to the SU in order to listen and add small interference noise power to the PU communication. If this method is not allowed by the PU, then we switch to the non-opportunistic mode of operation, which does not need obtaining the CSI between the TVWS BPLC Tx and the PU Rx.

As illustrated in Fig. 1, the binary encoded data is modulated using quadrature amplitude modulation (QAM) modulator. Each QAM symbol is precoded using either singular value decomposition (SVD) algorithm or projected singular value decomposition (P-SVD) algorithm. The precoding algorithm is discussed in detail in Section III. The received signal is decoded using a decoding matrix according to the precoding type. The decoded symbols are passed through a maximum likelihood (ML) detector to allow estimation of the transmitted symbols.

Since the proposed system accesses the TVWS, a cognitive spectrum access algorithm is proposed. In the algorithm the channel between a single TVWS BPLC Tx and Rx is considered to be $n_r \times n_r$ MIMO channel where n_r is the number of TVWS BPLC MIMO sub-channels as illustrated in Fig. 2. The n_r MIMO sub-channels are divided into two groups: 1) $(n_r-1)\times(n_r-1)$ MIMO BPLC sub-channels as in the case of 2×2 single phase MIMO BPLC and 3×3 three phase MIMO BPLC; 2) SISO TVWS wireless sub-channel. However, the channel between a TVWS BPLC Tx and a single TV PU Rx can be considered as $n_r \times 1$ MISO channel. This advantage is used by our proposed system for better TVWS BPLC to TV PU interference mitigation. The signal received at the TVWS BPLC Rx on subcarrier n can be represented as [20]

$$\mathbf{y}(n) = \tilde{\mathbf{H}}^{(n)}\mathbf{U}^{(n)}\mathbf{x}(n) + \mathbf{E}^{(n)}\mathbf{U}^{(n)}\mathbf{x}(n) + \mathbf{z}(n) \quad (1)$$

where $\tilde{\mathbf{H}}^{(n)}$ is the estimated $n_r \times n_r$ MIMO channel matrix for subcarrier n, which can be expressed as $\tilde{\mathbf{H}}^{(n)} = \mathbf{Q}^{(n)}(\mathbf{\Lambda}^{(n)})^{1/2}\mathbf{U}^{\dagger(n)}$. $\mathbf{E}^{(n)} = \mathbf{Q}^{(n)}\tilde{\mathbf{E}}^{(n)}\mathbf{U}^{\dagger(n)}$ is a zero mean Gaussian distributed error matrix with the variance σ_E^2, which represents the error introduced in the channel estimation as previously addressed in [21]–[23], the channel transfer matrix is assumed to be $\mathbf{H}^{(n)} = \tilde{\mathbf{H}}^{(n)} + \mathbf{E}^{(n)}$. $\mathbf{U}^{(n)}$ is the precoding matrix for subcarrier n and $\mathbf{z}(n)$ is additive white Gaussian noise (AWGN) vector whose elements have zero mean and variance σ_z^2. Without loss of generality, the antenna is assumed to be omnidirectional with unity gain [24], the directional antenna can further improve the performance by introducing more antenna gain.

Multiplying the received signal by the decoding matrix $\mathbf{Q}^{\dagger(n)}$, we have

$$\hat{\mathbf{y}}(n) = (\mathbf{\Lambda}^{(n)})^{1/2}\mathbf{x}(n) + \tilde{\mathbf{E}}^{(n)}\mathbf{x}(n) + \hat{\mathbf{z}}(n) \quad (2)$$

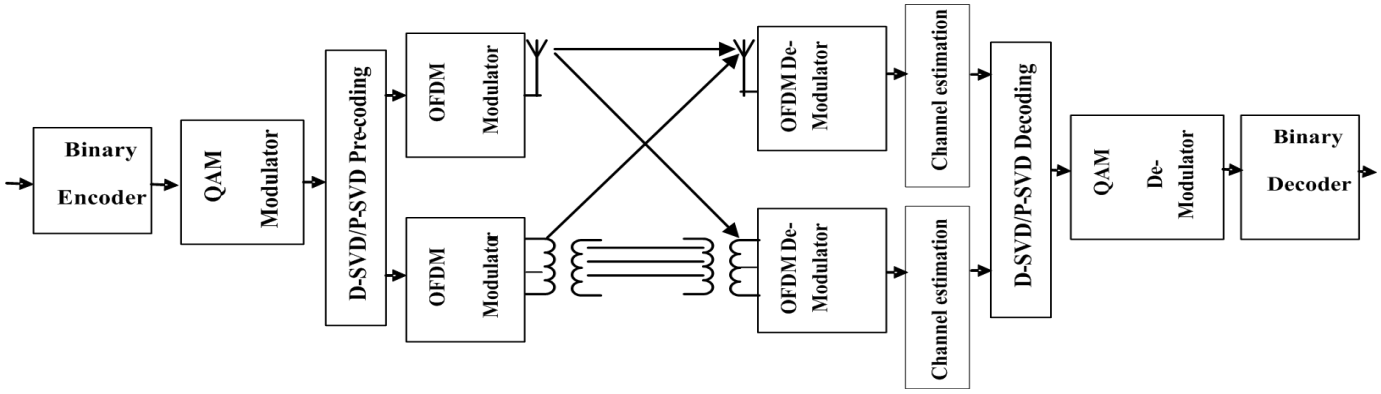

Fig. 1: System Model

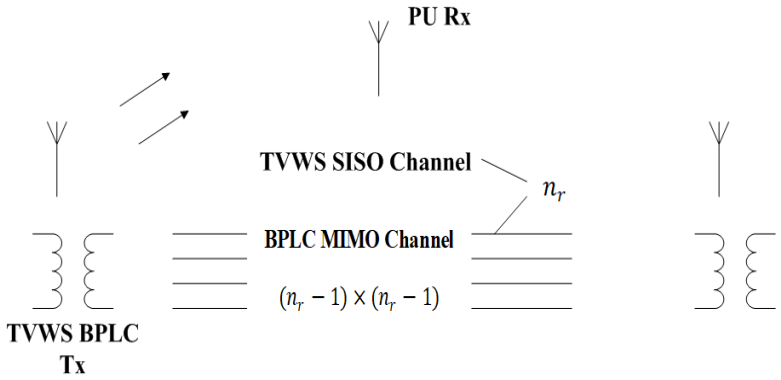

Fig. 2: $n_r \times n_r$ TVWS BPLC Tx-Rx channel model and $n_r \times 1$ TVWS BPLC Tx-TV PU Rx channel model

where $\hat{\mathbf{z}}(n) = \mathbf{Q}^{(n)}\mathbf{z}(n)$ and $\mathbf{\Lambda}^{(n)}$ is the matrix of the singular values of the MIMO channel power gain matrix $\mathbf{S}$ which can be defined as $\mathbf{S} = \tilde{\mathbf{H}}^{(n)}\tilde{\mathbf{H}}^{\dagger(n)}$.

B. Channel Models

In this paper, we are more focused on the relationship between the capacity of our proposed system and its coverage distance. Hence, we are interested in the average path loss as well as the complete channel gain between the TVWS BPLC Tx and Rx. The power line channel gain and its average path loss have been modelled in the VHF band in [25] for the nine classes of the power line channel [26]. In our research we consider class 1 power line channel that has been mostly measured and addressed in previous literature [12] [25] [27] [28]. In this paper, we further derive the empirical formula that describes class 1 average channel path loss model in Fig. 4 of our previous work [25]. The empirical formula can be represented as:

$$PL_{\mathrm{BPLC}}(dB) = (a_1 f^2 + a_2 f + a_3)d_e + (b_1 f^2 + b_2 f + b_3) \tag{3}$$

where f is the frequency of operation in MHz, d_e is the electric separation distance in meters, which is defined as the length of the power line cable between any BPLC Tx and Rx. $a_1 = -1.14 \times 10^{-4}$, $a_2 = 6.8 \times 10^{-3}$, $a_3 = -0.91$ and $b_1 = 2.97 \times 10^{-4}$, $b_2 = -0.061$, $b_3 = -15.0$. In our paper, we adopt the class 1 channel generator in [25] to generate random complex channel between the BPLC Tx and Rx.

Also, the wireless channel in the VHF band has been modelled in [16]. Hence, the TVWS-TVWS channel path loss can be represented as

$$PL_{\mathrm{TVWS}}(dB) = -10\log_{10}\left(\frac{\lambda_f}{4\pi d_0}\right)^{2.63} + 10l\log_{10}\frac{d_g}{d_0} + \alpha d_g + FAF \tag{4}$$

where d_g is the Tx-Rx geometric separation, d_0 is the close-in reference distance and it must be chosen to lie in the far field region (*i.e.*, $d_0 \gg \frac{\lambda_f}{2\pi}$, where the longest λ_f is 10 m at a frequency of 30 MHz), λ_f is the wavelength, l is the path loss exponent, α is the attenuation constant (dB/m) , and FAF is the floor attenuation factor. l,α and FAF take the values of 1.5, 0.65 and 0, respectively. We have chosen the floor attenuation to be zero, since TVWS and BPLC channels were measured on the same floor. This was forced by the restriction that the BPLC channel must be measured between outlets that belong to the same phase and distribution box to avoid interference between different phases. Each floor has a separate distribution box in the building of Electrical Engineering and Electronics, The University of Liverpool, where our measurements were conducted. In our paper we represent the indoor channel using 3 levels model, which considers three superimposed effects: 1) two-ray Rayleigh fading channel for the multipath effect

[29], with root mean square (rms) delay spread of 6 μs, 2) shadowing, and 3) path loss. Both shadowing and path loss effects are modeled using the VHF indoor path loss model in (4).

The noise model adopted in this paper has two components: 1) background noise: we consider additive white Gaussian background noise with zero mean and variance σ_z^2, and 2) impulsive noise, which is represented using the model in [30]. Also, the narrowband interference is considered in the form of PU interference with variance σ_p^2. More complex noise models such as the colored background noise models in [31] and [32] will be considered in our future work.

III. Cognitive Spectrum Access

In this section, the cognitive spectrum access for the hybrid TVWS BPLC Tx is presented, including: 1) An iterative precoding technique; 2) Cognitive spectrum sensing.

A. Iterative Hybrid SVD/P-SVD Precoding Technique

In our work, a new precoding algorithm is proposed for cognitive spectrum access. The algorithm aims to achieve maximum capacity while maintaining the interference limit at the TV PUs Rxs by applying Lemma 1 that will be discussed later in this Section. The algorithm precodes the TVWS BPLC Tx data according to the TVWS BPLC-TV PU channel. Two precoding algorithms are used: 1) SVD; 2) P-SVD [33]. The SVD is used in the idle channel case while a hybrid SVD/P-SVD is used in case of occupied channel. In case of SVD precoding, the channel matrix $\mathbf{H}^{(n)}$ is decomposed using SVD into $\mathbf{H}^{(n)} = \mathbf{Q}^{(n)}(\mathbf{\Lambda}^{(n)})^{1/2}\mathbf{U}^{\dagger(n)}$ where $\mathbf{Q}^{(n)}$ and $\mathbf{U}^{(n)}$ are $n_r \times n_r$ matrices with orthonormal columns. $\mathbf{\Lambda}^n$ is an $n_r \times n_r$ diagonal positive matrix with vector $\lambda^{(n)}$ as its diagonal. Hence, $\mathbf{V} = \mathbf{U}^{(n)}$ will be the precoding matrix as shown in (1). However, in the P-SVD precoding, the SU MIMO channel is first projected on to the null space of the interference channel vector with the PU. Then, the projected channel matrix is then decomposed using the SVD method. Let $\hat{\mathbf{g}_1}^{(n)} = \mathbf{g}_1^{(n)}/\|\mathbf{g}_1^{(n)}\|$ be the unit vector in the direction of $\mathbf{g}_1^{(n)}$ which represents the channel vector between the TVWS BPLC and the TV PUs. The subscript $1/0$ in $g_{1/0}^{(n)}$ indicates the TV PU presence/absence, respectively. We can define the projection of the channel matrix $\mathbf{H}^{(n)}$ in the null space of $\mathbf{g}_1^{\dagger(n)}$ as [33]

$$\mathbf{H}_{\perp}^{(n)} = \mathbf{H}^{(n)}(\mathbf{I} - \hat{\mathbf{g}_1}^{(n)}\hat{\mathbf{g}_1}^{\dagger(n)}) \tag{5}$$

The vector multiplication of $\hat{\mathbf{g}_1}^{(n)}\hat{\mathbf{g}_1}^{\dagger(n)}$ results in a matrix such that $(\hat{\mathbf{g}_1}^{(n)}\hat{\mathbf{g}_1}^{\dagger(n)})\hat{\mathbf{g}_1}^{(n)} = \hat{\mathbf{g}_1}^{(n)}$. Hence, $(\mathbf{I} - \hat{\mathbf{g}_1}^{(n)}\hat{\mathbf{g}_1}^{\dagger(n)})\hat{\mathbf{g}_1}^{(n)}$ is equal to zero. Consequently, $\mathbf{H}_{\perp}^{(n)}$ represents the projection of $\mathbf{H}^{(n)}$ matrix into the null space of $\hat{\mathbf{g}_1}^{\dagger(n)}$. Then using the SVD of $\mathbf{H}_{\perp}^{(n)} = \mathbf{Q}_{\perp}^{(n)}(\mathbf{\Lambda}_{\perp}^{(n)})^{1/2}\mathbf{U}_{\perp}^{\dagger(n)}$ we can conclude the precoding matrix $\mathbf{V} = \mathbf{U}_{\perp}^{(n)}$ and decode the received signal by multiplying by $\mathbf{Q}_{\perp}^{\dagger(n)}$.

$$\hat{\mathbf{y}}(n) = (\mathbf{\Lambda}_{\perp}^{(n)})^{1/2}\mathbf{x}(n) + \hat{\mathbf{z}}(n) \tag{6}$$

In our proposed precoding algorithm, both SVD and P-SVD are used jointly according to the CSI of both the TVWS BPLC and TV PU Rxs.

1) Idle Channel: In case of an idle channel, SVD is used as precoding scheme. Although the PU is absent, an interference limit is forced for false detection probability to avoid harmful interference. The TVWS BPLC-TV PU channel $\mathbf{g}_{0,k}^{(n)}$ with maximum gain $\max_{n_t} \|\mathbf{g}_{0,k}^{(n)}\mathbf{U}_0^{(n)}\|^2$ can only be accessed with power level below the interference limit where $k = 1, 2, ..n_t$ and n_t is the number of PUs.

2) Occupied Channel: This case is only applied to the opportunistic mode of operation mentioned in Section II. In this case, the PU is present, while the secondary user is allowed also to access the channel such that the received power at the TV PU Rx is below a certain interference limit Γ. In our proposed algorithm the SVD is also used as a default precoding scheme as in the case of the idle channel. However, the decision is taken to switch the precoding scheme to P-SVD according to the CSI of the TV PU Rx. The decision is taken to satisfy two conditions: 1) Achieve the interference limit at the TV PU Rx; 2) Achieve high SNR at the TVWS BPLC Rx. Hence, the previous two conditions can be satisfied knowing the CSI as follows. Let's assume that the interference limit is the minimum threshold for the signal to be detected by the Rx. Hence, the interference to the PU shall be below this threshold in order not to affect the PU reception, while the signal received at the TVWS BPLC Rx shall be above that threshold in order to be detected.

Lemma 1. Let γ be the signal to noise ratio (SNR) at the TVWS BPLC Rx and Γ be the interference limit at the TV PU Rx. In order to achieve $\gamma \geq \Gamma$ while satisfying the interference limit at the TV PU Rx, the following condition shall be satisfied

$$\det \begin{bmatrix} \frac{\lambda_1^{(n)}}{\rho} - \alpha_{1,k}^{(n)} & \dots & -\alpha_{n_r,k}^{(n)} \\ \vdots & & \vdots \\ -\alpha_{1,k}^{(n)} & \dots & \frac{\lambda_{n_r}^{(n)}}{\rho} - \alpha_{n_r,k}^{(n)} \end{bmatrix} \geq 0 \tag{7}$$

where the matrix diagonal is positive such that $\frac{\lambda^{(n)}}{\rho} \geq \alpha_{\mathbf{k}}{}^{(n)}$, ρ is a constant that satisfies $\rho \geq 1$ and $\alpha_k = \|\mathbf{g}_{1,k}^{(n)}\mathbf{U}_1^{(n)}\|^2$ of the k-th PU. Lemma 1 implies that the TVWS BPLC MIMO channel gain represented by its singular values $\lambda^{(n)}$ shall be greater than gain of the interference channel with the PU represented by α_k. The ρ constant controls the gap between both channel gains.

Proof. See Appendix A. □

Lemma 1 shall be satisfied for the use of SVD. If this condition is violated, then P-SVD is used to eliminate the interference at one TV PU Rx. The eliminated PU is selected to satisfy $\max_{n_t}\{\|\alpha_{\mathbf{k}}{}^{(n)}\|^2\}$. Hence, the algo-

rithm proposed for cognitive access can be summarized as

Proposed iterative hybrid SVD/P-SVD algorithm

- Initialize the precoding algorithm as SVD and $i = n_r$.
- While $i > 0$
  Check the condition in Lemma 1.
  - If the condition is satisfied, end the loop, otherwise change the precoding to P-SVD.
  - Select the TVWS BPLC-TV PU interference channel to be cancelled that satisfies $\max_{n_t}\{\|\alpha_{\mathbf{k}}{}^{(n)}\|\}$.
  - $i = i - 1$
- End.

B. Cognitive Spectrum Sensing

It is known that the sensing time is considered as a challenging issue for the cognitive systems. In our proposed system we achieve the optimum sensing time for a MIMO cognitive system through achieving the optimum detection probability for each MIMO sub-channel. This can be clarified in the following Lemma 2. Let $\hat{\mathcal{P}}_d$ represent the target detection probability of the MIMO cognitive Rx using the energy detection method. Also, let the OR rule (*i.e.*, the channel is detected occupied if the PU is detected using either the BPLC Rx or the TVWS Rx) be adopted for MIMO cognitive sensing. Hence, the relationship between the detection probability of each sub-channel and the target detection probability of the MIMO channel can be expressed as

Lemma 2.

$$\begin{aligned}&\Pi_{i=1}^{n_r}\Big(1-Q\Big[\frac{\gamma_m-\gamma_i}{\gamma_m\sqrt{2\gamma_i+1}}Q^{-1}(\hat{\mathcal{P}}_{fa})\\&+Q^{-1}(\mathcal{P}_{d_m})\sqrt{\frac{2\gamma_m+1}{2\gamma_i+1}}\Big]\Big)=1-\hat{\mathcal{P}}_d\end{aligned}\tag{8}$$

where $\mathcal{P}_{d_m}$ is the detection probability of the m-th MIMO sub-channel, γ_m and γ_i are the SNR of the m-th and i-th sub-channels, respectively for $i, m = 1, ..n_r$, $\hat{\mathcal{P}}_{fa}$ is the target false alarm of each MIMO sub-channel and $Q(.)$ is the complementary error function.

Proof. See Appendix B. □

Using Lemma 2, $\mathcal{P}_{d_m}$ can be derived numerically for any MIMO sub-channel. Let $N_{min} = \tau_{min} f_s$ be the minimum number of samples requested to achieve the target detection probability $\hat{P}_d$, f_s is the sampling frequency and τ_{min} is the minimum sensing time. N_{min} can be expressed as [34]

$$N_{min}=\frac{1}{\gamma_m^2}\Big(Q^{-1}(\mathcal{P}_{fa_m})-Q^{-1}(\mathcal{P}_{d_m})\sqrt{2\gamma_m+1}\Big)^2\tag{9}$$

N_{min} and τ_{min} can be directly evaluated after obtaining $\mathcal{P}_{d_m}$ numerically using Lemma 2.

IV. Capacity Maximization based Power Allocation

In this section, we present the capacity model and the power allocation algorithm that have been adopted to represent the MIMO TVWS BPLC channel.

A. Capacity Analysis

In [35], a system model was proposed for the cognitive spectrum access, where the secondary user could access the cognitive band with two power levels $P_0^{(n)}$ and $P_1^{(n)}$ in the TV PU absence and presence, respectively. In our work, we extend the algorithm in [35] to derive the allocated power for each sub-channel in a MIMO cognitive TVWS BPLC system, taking into consideration the use of SVD/P-SVD as a precoding technique. Also, the model is modified to represent the MISO interference channel between TVWS BPLC and TV PU. Hence, the spectral efficiencies (SEs) on the n-th subcarrier for the four scenarios are given as

$$r_{c,d}^{(n)}=\frac{1}{N}\Sigma_{i=1}^{n_r}\log_2\Big(1+\frac{\lambda_{d,i}^{(n)}P_{d,i}^{(n)}}{\sigma_z^2+\sigma_E^2P_{av}^{(n)}+d\sigma_p^2}\Big)\tag{10}$$

where c and d can take the values of 0 and 1 for the idle and occupied channel status, respectively. σ_z^2 and σ_p^2 are the noise power and the PU power, respectively. σ_E^2 is the variance of the channel estimation error $\mathbf{E}^{(n)}$ and $P_{av}^{(n)}$ is the maximum average power allowed for the TVWS BPLC Tx for subcarrier n. $\lambda_{d,i}^{(n)}$ and $P_{d,i}^{(n)}$ are the singular value and the TVWS BPLC Tx signal power of the i-th MIMO sub-channel and n-th subcarrier assigned to each detected channel status d.

Hence, we can conclude the MIMO ergodic SE as

$$\begin{aligned}R^{(n)}=&\frac{\Pi_{I0}}{N}\Big(\frac{T-\tau}{T}\Big)\mathbb{E}_{\mathbf{H}^{(n)},\mathbf{g}^{(n)}}\Big\{\mathcal{P}(H_0)(1-\mathcal{P}_{fa})r_{00}^{(n)}\\&+\mathcal{P}(H_0)\mathcal{P}_{fa}r_{01}^{(n)}+\mathcal{P}(H_1)(1-\mathcal{P}_d)r_{10}^{(n)}+\mathcal{P}(H_1)\mathcal{P}_dr_{11}^{(n)}\Big\}\end{aligned}\tag{11}$$

Hence, the overall capacity in (bits per seconds) for all the subcarriers can be expressed as

$$\begin{aligned}C=&\frac{B\Pi_{I0}}{N}\Big(\frac{T-\tau}{T}\Big)\Sigma_{n=1}^{N}\mathbb{E}_{\mathbf{H}^{(n)},\mathbf{g}^{(n)}}\Big\{\mathcal{P}(H_0)(1-\mathcal{P}_{fa})r_{00}^{(n)}\\&+\mathcal{P}(\mathcal{H}_0)\mathcal{P}_{fa}r_{01}^{(n)}+\mathcal{P}(\mathcal{H}_1)(1-\mathcal{P}_d)r_{10}^{(n)}+\mathcal{P}(\mathcal{H}_1)\mathcal{P}_dr_{11}^{(n)}\Big\}\end{aligned}\tag{12}$$

where $\mathcal{P}(\mathcal{H}_0)$ and $\mathcal{P}(\mathcal{H}_1)$ are the probabilities of TV PU absence and presence, respectively. $\mathcal{P}_d$ and $\mathcal{P}_{fa}$ are the TV PU detection probability and false alarm probability, respectively. T is the symbol time duration and τ is the TV PU detection time duration. Π_{I0} is the steady-state probability of the non-burst impulsive state $I0$ of the BPLC channel [30]. It is worth mentioning that due to low occurrence probability of impulsive bursts, Π_{I0} can take values which are close to one [30]. B is the total channel bandwidth of the OFDM symbol and N is the total number of subcarriers. For a constrained power communication system, the average MIMO power of

the TVWS BPLC per subcarrier shall be less than a pre-defined value P_{av} as

$$\mathbb{E}_{\mathbf{H}^{(n)},\mathbf{g}^{(n)}}\{\mathcal{P}(\mathcal{H}_0)(1-\mathcal{P}_{fa})\Sigma_{i=1}^{n_r}P_{0,i}^{(n)}+\mathcal{P}(\mathcal{H}_0)\mathcal{P}_{fa}\Sigma_{i=1}^{n_r}P_{1,i}^{(n)} +\mathcal{P}(\mathcal{H}_1)(1-\mathcal{P}_d)\Sigma_{i=1}^{n_r}P_{0,i}^{(n)}+\mathcal{P}(\mathcal{H}_1)\mathcal{P}_d\Sigma_{i=1}^{n_r}P_{1,i}^{(n)}\}\leq P_{av} \tag{13}$$

Also, the MISO interference of each subcarrier to the TV PU is limited to a certain value Γ as

$$\mathbb{E}_{\mathbf{H}^{(n)},\mathbf{g}^{(n)}}\{\mathcal{P}(\mathcal{H}_1)(1-\mathcal{P}_d)\|\mathbf{g}_0^{(n)}\mathbf{U}_0^{(n)}\|^2\mathbf{P}_0^{(n)} +\mathcal{P}(\mathcal{H}_1)\mathcal{P}_d\|\mathbf{g}_1^{(n)}\mathbf{U}_1^{(n)}\|^2\mathbf{P}_1^{(n)}\}\leq\Gamma \tag{14}$$

$\mathbf{U}_0^{(n)}$ and $\mathbf{U}_1^{(n)}$ are the precoding matrices in case of TV PU absence and TV PU presence, respectively. Also $\mathbf{g}_0^{(n)}$ and $\mathbf{g}_1^{(n)}$ are the selected TVWS BPLC-TV PU channel gain for the cases of TV PU absence and presence, respectively. The criterion of selection is according to the precoding scheme as mentioned in Section III. $\mathbf{P}_0^{(n)}$ and $\mathbf{P}_1^{(n)}$ are the TVWS BPLC signal power vectors in case of TV PU absence and presence, respectively where $P_{0,i}^{(n)}$ and $P_{1,i}^{(n)}$ are their i-th elements, respectively.

B. Power Allocation

In [35] a power allocation algorithm was proposed for SISO cognitive system. In our work, we extend the algorithm in [35] to derive the allocated power for each sub-channel in a MIMO cognitive TVWS BPLC system, taking into consideration the use of SVD/P-SVD as a precoding technique. The power is allocated to each sub-channel in both cases of TV PU presence and absence. The power allocation is done in a way to maximize the TVWS BPLC MIMO capacity for each subcarrier and satisfy both TVWS BPLC average power and TV PU Rx interference power limit. Hence, the problem of allocating the power can be formulated as

$$\max_{P_{0,i}^{(n)},P_{1,i}^{(n)}}(R^{(n)})=\Big(\frac{T-\tau}{T}\Big)\mathbb{E}_{\mathbf{H}^{(n)},\mathbf{g}^{(n)}}\{\mathcal{P}(\mathcal{H}_0)(1-\mathcal{P}_{fa})r_{00}^{(n)} +\mathcal{P}(\mathcal{H}_0)\mathcal{P}_{fa}r_{01}^{(n)}+\mathcal{P}(\mathcal{H}_1)(1-\mathcal{P}_d)r_{10}^{(n)}+\mathcal{P}(\mathcal{H}_1)\mathcal{P}_d r_{11}^{(n)}\} \tag{15}$$

Subject to (13), (14) and $P_{0,i}^{(n)},P_{1,i}^{(n)}\geq 0$, where the $\frac{\Pi_{I0}}{N}$ is omitted to simplify the derivation. The dual Lagrangian function can be represented as

$$\begin{aligned}&L(P_{0,i}^{(n)},P_{1,i}^{(n)},u,v)= \\ &\Big(\frac{T-\tau}{T}\Big)\mathbb{E}_{\mathbf{H}^{(n)},\mathbf{g}^{(n)}}\{\mathcal{P}(\mathcal{H}_0)(1-\mathcal{P}_{fa})r_{00}^{(n)}+\mathcal{P}(\mathcal{H}_0)\mathcal{P}_{fa}r_{01}^{(n)} \\ &+\mathcal{P}(\mathcal{H}_1)(1-\mathcal{P}_d)r_{10}^{(n)}+\mathcal{P}(\mathcal{H}_1)\mathcal{P}_d r_{11}^{(n)}\}-v\mathbb{E}_{\mathbf{H}^{(n)},\mathbf{g}^{(n)}}\{ \\ &\mathcal{P}(\mathcal{H}_0)(1-\mathcal{P}_{fa})\Sigma_{i=1}^{n_r}P_{0,i}^{(n)}+\mathcal{P}(\mathcal{H}_0)\mathcal{P}_{fa}\Sigma_{i=1}^{n_r}P_{1,i}^{(n)} \\ &+\mathcal{P}(\mathcal{H}_1)(1-\mathcal{P}_d)\Sigma_{i=1}^{n_r}P_{0,i}^{(n)}+\mathcal{P}(\mathcal{H}_1)\mathcal{P}_d\Sigma_{i=1}^{n_r}P_{1,i}^{(n)}\} \\ &+vP_{av}-u\mathbb{E}_{\mathbf{H}^{(n)},\mathbf{g}^{(n)}}\{\mathcal{P}(\mathcal{H}_1)(1-\mathcal{P}_d)\|\mathbf{g}_0^{(n)}\mathbf{U}_0^{(n)}\|^2\mathbf{P}_0^{(n)} \\ &+\mathcal{P}(\mathcal{H}_1)\mathcal{P}_d\|\mathbf{g}_1^{(n)}\mathbf{U}_1^{(n)}\|^2\mathbf{P}_1^{(n)}\}+u\Gamma\end{aligned} \tag{16}$$

The dual problem can be represented as

$$d(v,u)=\sup_{P_{0,i}^{(n)},P_{1,i}^{(n)}}L(P_{0,i}^{(n)},P_{1,i}^{(n)},u,v) \tag{17}$$

In order to obtain the supremum of the Langrangian with respect to the transmission powers we can use the primal dual decomposition. Let $i\in 1,2,..,n_r$ be an index for the MIMO sub-channel and $j\in 0,1$ be an index for the TV PU status (*i.e.*, 0 in case of absence and 1 in case of presence). Also, let $\eta_0=\mathcal{P}(\mathcal{H}_0)(1-\mathcal{P}_{fa})$, $\eta_1=\mathcal{P}(\mathcal{H}_0)\mathcal{P}_{fa}$, $\beta_0=\mathcal{P}(\mathcal{H}_1)(1-\mathcal{P}_d)$ and $\beta_1=\mathcal{P}(\mathcal{H}_1)\mathcal{P}_d$. Using the primal dual decomposition, we can subdivide the joint variable optimization problem into $n_r\times 2$ single variable convex optimization problems as

$$\begin{aligned}&\max_{P_{j,i}^{(n)}\geq 0}(f(P_{j,i}^{(n)}))=\Big(\frac{T-\tau}{T}\Big)\mathbb{E}_{\mathbf{H}^{(n)},\mathbf{g}^{(n)}}\{\eta_j r_{0j,i}^{(n)}+\beta_j r_{1j,i}^{(n)}\} \\ &-v\mathbb{E}_{\mathbf{H}^{(n)},\mathbf{g}^{(n)}}\{(\eta_j+\beta_j)P_{j,i}^{(n)}\}-u\mathbb{E}_{\mathbf{H}^{(n)},\mathbf{g}^{(n)}}\{\beta_j\alpha_{j,i,k}^{(n)}P_{j,i}^{(n)}\}\end{aligned} \tag{18}$$

Using the subgradient method, the solution to each problem can be addressed as

$$P_{j,i}^{(n)}=\lceil A_{i,j}+\sqrt{B_{i,j}}\rceil^{+} \tag{19}$$

where

$$A_{i,j}=\frac{\Big(\frac{T-\tau}{T}\Big)\log_2(e)(\eta_j+\beta_j)}{v(\eta_j+\beta_j)+u\beta_j\alpha_{j,i,k}^{(n)}}+\frac{2(\sigma_z^2+\sigma_E^2P_{av}^{(n)})+\sigma_p^2}{\lambda_{j,i}^{(n)}} \tag{20}$$

$$\begin{aligned}B_{i,j}=A_{i,j}^2-\frac{4}{\lambda_{j,i}^{(n)}}\Big[\frac{(\sigma_z^2+\sigma_E^2P_{av}^{(n)})+\sigma_p^2}{\lambda_{j,i}^{(n)}\sigma_p^2}- \\ \frac{\Big(\frac{T-\tau}{T}\Big)\log_2(e)(\eta_j((\sigma_z^2+\sigma_E^2P_{av}^{(n)})+\sigma_p^2)+\beta_j(\sigma_z^2+\sigma_E^2P_{av}^{(n)}))}{v(\eta_j+\beta_j)+u\beta_j\alpha_{j,i,k}^{(n)}}\Big]\end{aligned} \tag{21}$$

V. Simulation Results

A. Simulation Setup

In this section, the simulation results are presented for our proposed system compared to the MIMO BPLC [4] and the BPLC WiFi [12]. The OFDM symbol duration T is taken to be 5 ms. It is assumed that the BPLC channel as well as its noise has cyclostationary behavior with a coherence time which is typically half of the mains period (*i.e.*, 10 ms) [3]. For the VHF wireless channel, we assume a Rayleigh fading channel with average path loss as in (4), the l, α and d_0 are set to 1.5, 0.65 and 12 m, respectively [16]. The total bandwidth from 54 MHz to 88 MHz is divided into 5 channels. Each channel has 6 MHz bandwidth. The transmission PSDs for the TVWS BPLC, MIMO BPLC and BPLC WiFi are set to -47 dBm/Hz, -85 dBm/Hz and -50 dBm/Hz, respectively. The received SNR (*i.e.*, the ratio of the received signal power to the power sum of the AWGN and the channel estimation error variance, regardless of the PU interference power) varies from 20 dB to 40 dB. The requested probability of false alarm and detection probability are 10^{-7} and 0.9999, respectively. Also,

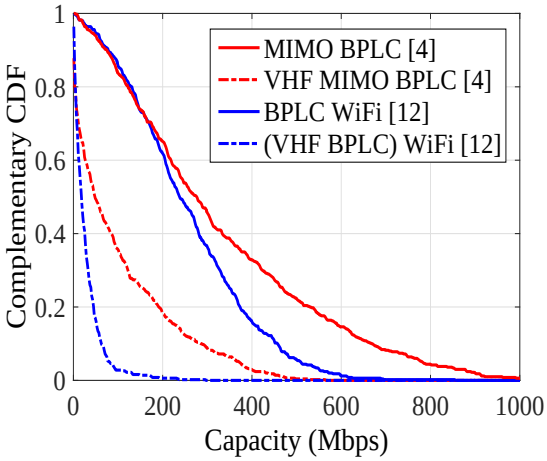

Fig. 3: Complementary CDF vs. ergodic capacity at different frequency bands

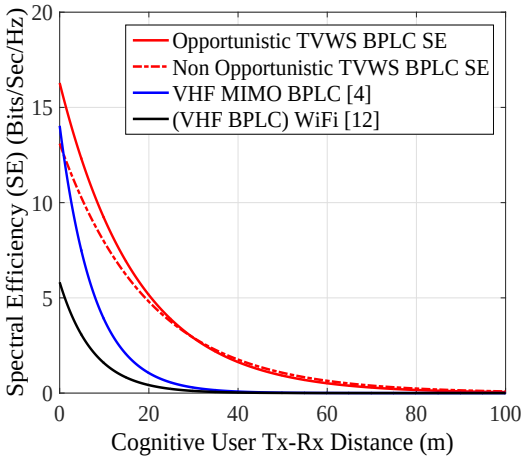

Fig. 4: Average cognitive user SE vs. Tx-Rx distance

the probability of TV PU presence is 0.4. The received PU SNR is assumed to be -14 dB. n_r and n_t are assumed to be equal 2. Also, energy detection algorithm is adopted for cognitive sensing and the OR-rule technique is adopted for MIMO sensing.

For the simulation of the power line environment, we use the random topology generator presented in [36]. Each iteration, a random power line topology is generated and 4 points are randomly selected to represent TVWS BPLC Tx and Rx and two TV PU Rxs.

B. Simulation Results

1) Capacity and spectral efficiency at different frequency bands coverage: In Fig. 3, the capacity complementary cumulative distribution function (CCDF) of the MIMO BPLC [4] and the BPLC WiFi [12] is compared for different frequency bands. The degradation in the performance is observed in the case of using VHF BPLC compared to the conventional BPLC. In the conventional BPLC, both the high frequency (HF) band below 30 MHz and the VHF band are allowed. Hence, more transmission power can be allocated to the HF band of the conventional BPLC leading to more capacity compared to the VHF BPLC.

2) TVWS BPLC spectral efficiency: In Fig. 4, the average SE of our proposed system is compared to the MIMO BPLC [4] and the BPLC WiFi [12] in the VHF band. Two notable observations can be addressed: First, our proposed system significantly improves the SE compared to the MIMO BPLC and the BPLC WiFi. This is due to compliance with the TVWS standard, which allows a transmission power of 100 mW per 6 MHz channel and yet a PSD of -47 dBm/Hz. This yields a 38 dB increase in the PSD in the VHF band compared to the IEEE 1901 standard used in the MIMO BPLC. Also, the VHF band has better channel gain than the 2.45 GHz band used in the BPLC WiFi. Second, a slight degradation in the performance in the TVWS BPLC for the non opportunistic case compared to the opportunistic case. This is due to the PU user interference in the opportunistic case that decreases the achievable capacity in the presence of the PU.

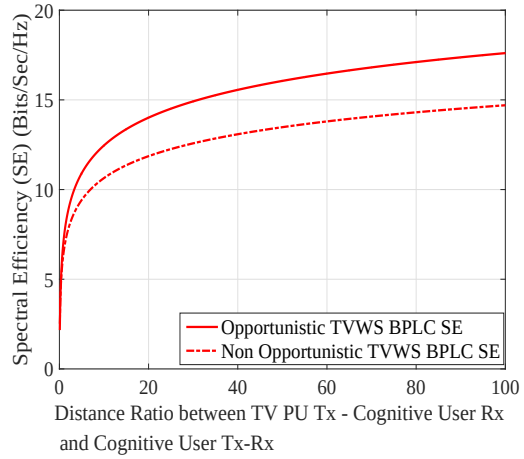

Fig. 5: Average cognitive user SE vs. the ratio between the TV PU Rx cognitive user Tx distance and the cognitive user Tx-Rx distance

In Fig. 5, our proposed TVWS BPLC SE shows a rapid saturation to the maximum as the distance ratio increases. This proves that our proposed system including the two modes of operation are less interfering to the PU Rx even if they are located at very close distance to the PU Rx. This is due to the use of our proposed iterative precoding algorithm that has the ability to mitigate the interference with the nearby TV PU Rx. The figure also reflects a slower increase in the SE for distance ratios above 3. However, the SE curve does not reach a saturation point until a distance ratio value becomes 100. This is because the distance ratio is bounded by the small areas inside the indoor environment. Hence, the TV PU Rx distance from our TVWS BPLC Tx is in the range of few tens of meters, which could limit the TVWS BPLC Tx transmission power and its spectral efficiency to avoid interference with

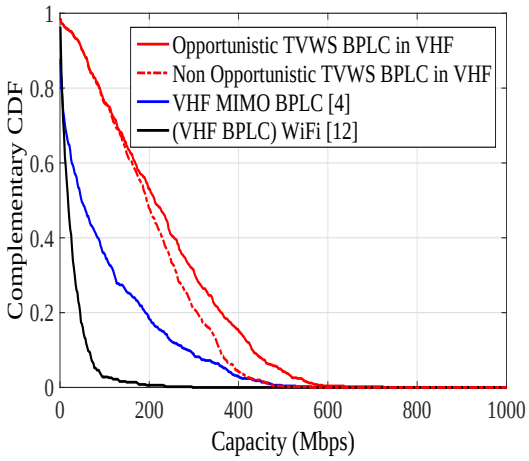

Fig. 6: Complementary CDF vs. ergodic capacity in the VHF band

the TV PU Rx. Hence, as the indoor distance between the TV PU Rx and the TVWS BPLC Tx increases, the TVWS BPLC spectral efficiency increases.

3) Ergodic capacity of the VHF band: In this part, we compute the ergodic capacity for the VHF band between 54 MHz and 88 MHz.

In Fig. 6, the complementary cumulative distribution function (CCDF) is presented versus the capacity. It can be observed that for the conventional cognitive BPLC system less than 0.2 % of the users can achieve 200 Mbps, for the BPLC WiFi 10% can achieve the 200 Mbps and for the MIMO BPLC 30% can achieve the same capacity. However, for our proposed system more than 95 % of the users can achieve 200 Mbps and more than 50 % can achieve 400 Mbps.

VI. Conclusion

In this paper, a novel hybrid TVWS BPLC system has been proposed for the indoor communication networks. The proposed system offers a cost-effective solution for enhancing the BPLC capacity in the VHF band. Also, an iterative precoding algorithm has been proposed to mitigate the interference with the TV PU Rxs in the VHF band. Moreover, a MIMO power allocation algorithm has been developed for the cognitive radio system. Through simulations it has been shown that our proposed system improves the BPLC capacity significantly. In the simulations, a single BPLC subchannel has been considered to form a 2×2 TVWS BPLC system. The capacity of the proposed system can be further enhanced by using MIMO BPLC together with the TVWS wireless channel. We have also shown that the capacity enhancement has been preserved under small separation distances from the TV PU Rx. Moreover, the proposed system demonstrates robust performance against the variation in the BPLC coupling loss which affects the cognitive BPLC sensing time and capacity in the VHF band.

Appendix A: Proof of Lemma 1

Let $\alpha_{i,k}^{(n)}$ be the i-th component of the interference vector α_k. In order to satisfy the interference power limit at the TV PU Rx, while maintaining good SNR at the Rx

$$\Sigma_{i=1}^{n_r} \alpha_{i,k}^{(n)} P_{i,k}^{(n)} \leq \Gamma, \quad \mathbf{\Lambda}^{(n)} \mathbf{P}_1^{(n)} \succeq \sigma_n^2 + \sigma_p^2 \tag{22}$$

Let $\Gamma \leq \sigma_n^2$ to avoid harmful interference. Also let $\sigma_n^2 + \sigma_p^2 = \rho\Gamma$. Hence, the following equation can be concluded

$$\mathbf{\Lambda}^{(n)} \mathbf{P}_1^{(n)} \succeq \rho \alpha_k^{(n)} \mathbf{P}_1^{(n)} \tag{23}$$

This can be translated in the following matrix form

$$\begin{bmatrix} \frac{\lambda_1^{(n)}}{\rho} - \alpha_{1,k}^{(n)} & \dots & -\alpha_{n_r,k}^{(n)} \\ \vdots & & \vdots \\ -\alpha_{1,k}^{(n)} & \dots & \frac{\lambda_{n_r}^{(n)}}{\rho} - \alpha_{n_r,k}^{(n)} \end{bmatrix} \begin{bmatrix} P_1^{(n)} \\ \vdots \\ P_{n_r}^{(n)} \end{bmatrix} \succeq 0 \tag{24}$$

Directly, the condition in (7) can be concluded.

Appendix B: Proof of Lemma 2

Using the OR decision rule for MIMO channel we get

$$\hat{\mathcal{P}}_d = 1 - \Pi_{i=1}^{n_r} (1 - \mathcal{P}_{d_i}) \tag{25}$$

where $\mathcal{P}_{d_i}$ can be expressed as follows for the energy detection method [34]

$$\mathcal{P}_{d_i} = Q\Big((\frac{\epsilon}{\sigma_n^2} - \gamma_i - 1) \Big(\sqrt{\frac{\tau_i f_s}{2\gamma_i + 1}} \Big) \Big) \tag{26}$$

where ϵ is the detection threshold. N_{min} is assumed to be equal for all the MIMO sub-channels. Hence, relationship between the detection probabilities of two MIMO sub-channels i and m can be expressed as follows using (9)

$$\mathcal{P}_{d_i} = Q\Big(\frac{\gamma_m - \gamma_i}{\gamma_m \sqrt{2\gamma_i + 1}} Q^{-1}(\hat{\mathcal{P}}_{fa}) + Q^{-1}(\mathcal{P}_{d_m}) \sqrt{\frac{2\gamma_m + 1}{2\gamma_i + 1}} \Big) \tag{27}$$

Substituting (27) into (25), we can directly get Lemma 2.

References

[1] M. U. Rehman, S. Wang, Y. Liu, S. Chen, X. Chen, and C. G. Parini, "Achieving high data rate in multiband-OFDM UWB over power-line communication system," *IEEE Transactions on Power Delivery*, vol. 27, no. 3, pp. 1172–1177, July 2012.

[2] M. Karduri, M. D. Cox, and N. J. Champagne, "Near-field coupling between broadband over power line (BPL) and high-frequency communication systems," *IEEE Transactions on Power Delivery*, vol. 21, no. 4, pp. 1885–1891, October 2006.

[3] H. C. Ferreira, L. Lampe, J. Newbury, T. Swart, and Editors, *Power Line Communications: Theory and Applications for Narrowband and Broadband Communications over Power Lines*. John Wiley & Sons, Inc., 2010.

[4] L. T. Berger, A. Schwager, P. Pagani, and D. Schneider, *MIMO Power Line Communications: Narrow and Broadband Standards, EMC, and Advanced Processing*. CRC Press, 2014.

[5] I. S. Association *et al.*, "IEEE Standard for Broadband over Power Line Networks: Medium Access Control and Physical Layer Specifications," *IEEE Std 1901*, vol. 2010, pp. 1–1586, 2010.

[6] N. Weling, "SNR-based detection of broadcast radio stations on power-lines as mitigation method toward a cognitive PLC solution," in *Proc. 16th IEEE International Symposium on Power Line Communications and Its Applications (ISPLC)*, pp. 52–59, March 2012, Beijing, China.

[7] R. Vuohtoniemi, J.-P. Makela, J. Vartiainen, and J. Iinatti, "Detection of broadcast signals in cognitive radio based PLC using the FCME algorithm," in *Proc. IEEE International Symposium on Power Line Communications and its Applications (ISPLC)*, pp. 70–74, March 2014, Glasgow, Scotland.

[8] B. Praho, M. Tlich, P. Pagani, A. Zeddam, and F. Nouvel, "Cognitive detection method of radio frequencies on power line networks," in *Proc. IEEE International Symposium on Power Line Communications and Its Applications (ISPLC)*, pp. 225–230, March 2010, Rio de Janeiro, Brazil.

[9] K. M. Ali, G. G. Messier, and S. W. Lai, "DSL and PLC co-existence: An interference cancellation approach," *IEEE Transactions on Communications*, vol. 62, no. 9, pp. 3336–3350, September 2014.

[10] S. W. Oh, Y. L. Chiu, K. N. Ng, R. Mo, Y. Ma, Y. Zeng, and A. Syed Naveen, "Cognitive power line communication system for multiple channel access," in *Proc. IEEE International Symposium on Power Line Communications and Its Applications*, pp. 47–52, March 2009, Dresden, Germany.

[11] J. Maes, M. Timmers, and M. Guenach, "Spectral compatibility of in-home and access technologies," in *Proc. IEEE International Symposium on Power Line Communications and Its Applications (ISPLC)*, pp. 7–11, April 2011, Udine, Italy.

[12] S. W. Lai, N. Shabehpour, G. G. Messier, and L. Lampe, "Performance of wireless/power line media diversity in the office environment," in *Proc. IEEE Global Communications Conference (GLOBECOM)*, pp. 2972–2976, December 2014, Texas, USA.

[13] B. O'hara and A. Petrick, *IEEE 802.11 handbook: a designer's companion*. IEEE Standards Association, 2005.

[14] "Second Report and Order and Memorandum Opinion and Order In the Matter of Unlicensed Operation in the TV Broadcast Bands, Additional Spectrum for Unlicensed Devices Below 900 MHz and in the 3 GHz Band," *Federal Communication Commision, Document 08-260*, November 2008.

[15] A. H. Ali, M. A. Razak, M. Hidayab, S. A. Azman, M. Z. M. Jasmin, and M. A. Zainol, "Investigation of indoor WIFI radio signal propagation," in *Proc. IEEE Symposium on Industrial Electronics & Applications (ISIEA) 2010*, pp. 117–119, October 2010, Penang, Malaysia.

[16] J. Andrusenko, R. L. Miller, J. A. Abrahamson, N. M. Merheb Emanuelli, R. S. Pattay, and R. M. Shuford, "VHF general urban path loss model for short range ground-to-ground communications," *IEEE Transactions on Antennas and Propagation*, vol. 56, no. 10, pp. 3302–3310, October 2008.

[17] M. Fadda, M. Murroni, and V. Popescu, "A cognitive radio indoor HDTV multi-vision system in the TV white spaces," *IEEE Transactions on Consumer Electronics*, vol. 58, no. 2, pp. 302–310, May 2012.

[18] M. Heggo, X. Zhu, Y. Huang, and S. Sun, "A Hybrid Power Line and TV White Space MIMO System for Indoor Broadband Communications," in *Proc. IEEE 84th Vehicular Technology Conference (VTC)*, September 2016, Montreal, Canada.

[19] A. Jovicic and P. Viswanath, "Cognitive radio: An information-theoretic perspective," *IEEE Transactions on Information Theory*, vol. 55, no. 9, pp. 3945–3958, September 2009.

[20] T. Yoo and A. Goldsmith, "Capacity and power allocation for fading MIMO channels with channel estimation error," *IEEE Transactions on Information Theory*, vol. 52, no. 5, pp. 2203–2214, May 2006.

[21] S. J. Grant and J. K. Cavers, "Performance enhancement through joint detection of cochannel signals using diversity arrays," *IEEE Transactions on Communications*, vol. 46, no. 8, pp. 1038–1049, August 1998.

[22] X. Zhu and R. D. Murch, "Performance analysis of maximum likelihood detection in a mimo antenna system," *IEEE Transactions on Communications*, vol. 50, no. 2, pp. 187–191, February 2002.

[23] R. H. Etkin and D. N. Tse, "Degrees of freedom in some underspread MIMO fading channels," *IEEE Transactions on Information Theory*, vol. 52, no. 4, pp. 1576–1608, April 2006.

[24] J. Davies, *Newnes Radio Engineer's Pocket Book*. Elsevier, 2014.

[25] M. Heggo, X. Zhu, Y. Huang, and S. Sun, "A novel statistical approach of path loss mapping for indoor broadband power line communications," in *Proc. IEEE International Conference on Smart Grid Communications (SmartGridComm) 2014*, pp. 499–504, November 2014, Venice, Italy.

[26] M. Tlich, A. Zeddam, F. Moulin, and F. Gauthier, "Indoor power-line communications channel characterization up to 100 MHzpart I: one-parameter deterministic model," *IEEE Transactions on Power Delivery*, vol. 23, no. 3, pp. 1392–1401, July 2008.

[27] Z. Tao, Y. Xiaoxian, and Z. Baohui, "Broadband transmission characteristics for power-line channels," *IEEE transactions on power delivery*, vol. 21, no. 4, pp. 1905–1911, October 2006.

[28] F. Versolatto and A. M. Tonello, "On the relation between geometrical distance and channel statistics in in-home plc networks," in *Proc. 16th IEEE International Symposium on Power Line Communications and Its Applications (ISPLC)*, pp. 280-285, March 2012, Beijing, China.

[29] N. Benvenuto and L. Tomba, "Performance comparison of space diversity and equalization techniques for indoor radio systems," *IEEE transactions on vehicular technology*, vol. 46, no. 2, pp. 358–368, May 1997.

[30] J. Yin, X. Zhu, and Y. Huang, "Modeling of amplitude-correlated and occurrence-dependent impulsive noise for power line communication," in *Proc. IEEE International Conference on Communications (ICC)*, pp. 4565–4570, June 2014, Sydney, Australia.

[31] H. Meng, Y. L. Guan, and S. Chen, "Modeling and Analysis of Noise Effects on Broadband Power-Line Communications," *IEEE Transactions on Power delivery*, vol. 20, no. 2, pp. 630–637, April 2005.

[32] J. Song, Q. Wu, C. Pan, Z. Yang, H. Liu, B. Zhao, and X. Li, "Two-way digital video transmission over medium-voltage power-lines using time-domain synchronous orthogonal frequency division multiplexing technology," *Tsinghua Science & Technology*, vol. 13, no. 6, pp. 784–789, December 2008.

[33] R. Zhang and Y.-C. Liang, "Exploiting multi-antennas for opportunistic spectrum sharing in cognitive radio networks," *IEEE Journal of Selected Topics in Signal Processing*, vol. 2, no. 1, pp. 88–102, February 2008.

[34] Y.-C. Liang, Y. Zeng, E. C. Peh, and A. T. Hoang, "Sensing-throughput tradeoff for cognitive radio networks," *IEEE Transactions on Wireless Communications*, vol. 7, no. 4, pp. 1326–1337, April 2008.

[35] S. Stotas and A. Nallanathan, "Enhancing the capacity of spectrum sharing cognitive radio networks," *IEEE Transactions on Vehicular Technology*, vol. 60, no. 8, pp. 3768–3779, October 2011.

[36] A. M. Tonello and F. Versolatto, "Bottom-up statistical PLC channel modelingPart I: Random topology model and efficient transfer function computation," *IEEE Transactions on Power Delivery*, vol. 26, no. 2, pp. 891–898, April 2011.